ELSEVIER

Journal of Organometallic Chemistry 551 (1998) 299–311

Journal of Organometallic Chemistry

The effect of low molecular weight organosiloxane substituents on mesophase formation and structure in non-symmetric nickel(II) complexes [1]

Isabel M. Saez, Georg H. Mehl, Ekkehard Sinn, Peter Styring *

Department of Chemistry, The University of Hull, Hull, HU6 7RX, UK

Received 6 June 1997

Abstract

Organosiloxane groups have been used as components of metal-containing liquid crystals (metallomesogens). It has been found that the disiloxane unit aids mesophase formation, stabilising an enantiotropic smectic A phase over a wide temperature range. The overall effect of an organodisiloxane unit is to lower the melting point relative to an alkyl substituted complex while increasing the clearing temperature, or leaving it unchanged, and so increasing mesophase temperature range. A model for the mesophase is proposed based on thermo-optical polarized light microscopy and small angle X-ray scattering studies. This proposes that weak nickel–nickel interactions, which are observed in the solid state, are maintained in the mesophase. The unusual steric shape of the organosiloxane group stabilizes the smectic A structure, allowing more efficient packing of the flexible chains. © 1998 Elsevier Science S.A.

Keywords: Organosiloxanes; Metallomesogens; Self-assembly; Thermo-optic properties

1. Introduction

Metal-containing liquid crystals (metallomesogens) have attracted considerable interest in recent years [1]. However, one of the major drawbacks that precludes the application of metallomesogens in practical electro-optic devices are the high melting points and clearing points of the complexes. In organic liquid crystal chemistry, the use of a pentamethyldisiloxane (PMDS) terminal group leads to significant decreases in the melting points of the materials while, in general, the effect on the clearing temperatures has been found to depend on the type of mesogenic group employed [2,3]. The result is a wide liquid crystal phase range with a mesophase that is stable at room temperature. This effect has been attributed to aggregation of like segments within the molecular structure to form segregated layers, assuming that the molecule is composed of a polar aromatic core, a non-polar hydrocarbon chain and a polar yet distinct PMDS terminal unit [3,4]. The phase behavior of these low molar mass siloxanes is similar to that of polymeric liquid crystalline siloxanes with respect to their solid and condensed phase behavior [3,4].

We have shown that it is possible to synthesize mono-activated, non-symmetric liquid crystalline co-ordination complexes that can be easily polymerized [5] or hydrosilylated [5–7]. Using the latter methodology, it is possible to obtain organosiloxane materials using a wide variety of silicon-containing precursors. In this paper the synthesis of an organosiloxane-terminated nickel-containing metallomesogens, and analogous complexes containing only hydrocarbon terminal chains, will be discussed and their thermal and optical behavior will be evaluated. Small angle X-ray scattering (SAXS) studies have been undertaken in order to elucidate the role of the organosiloxane unit in the molecular structure of the mesophase. A model for the mesophase structure in these unique materials is also suggested.

* Corresponding author. Tel: +44-0148-246-5409; fax: +44-0148-246-6411; e-mail: p.styring@chem.hull.ac.uk.

[1] Dedicated to Professor Peter Maitlis on the occasion of his 65th birthday.

2. Results and discussion

2.1. Synthesis

(4-Hydroxyphenyl)dimethylaminoacrolein (**1**) was prepared by the Vilsmeier–Arnold–Haack formylation of commercial (4-hydroxyphenyl)acetic acid as described by Lloyd et al. [8]. 2-(4-Decyloxyphenyl)-*N*,*N*-dimethyl-1-aminoprop-1-en-3-al (**2**) was prepared (Scheme 1) by standard alkylation of **1** with 1-bromodec-10-ene. Hydrolysis of **2** in strong, aqueous sodium hydroxide followed by acidification yielded the desired (4-decenyloxyphenyl) malonaldehyde (**3b**).

The unsymmetrical ligands (**6**) were prepared by the reaction of equimolar quantities of an appropriate phenylmalonaldehyde (**3**), an appropriate salicylaldehyde (**5**) and 1,2-diaminoethane in dichloromethane under reflux with the separation of water (Scheme 2). The ^{1}H NMR spectra of the ligands exhibit four unique resonances in the region 13.5 to 7.5 ppm, which have been assigned to the four different protons in the non-symmetrical NN′OO′ chelating core. The asymmetry of the ligand is also reflected in the ethylenediamine region which shows two distinct resonances at around 3.8 and 3.65 ppm. The unsymmetrical, diamagnetic, square-planar nickel(II) complexes (**7–9**) were obtained by the reaction of equimolar quantities of nickel acetate tetrahydrate and an appropriate ligand (**6**) in refluxing methanol. Materials were characterized by standard spectroscopic techniques (IR; MS (EI and FAB); ^{1}H NMR) and by elemental analysis. In some cases (e.g. **9**), a methanol of crystallisation was observed in the resulting complex.

The pentamethyldisiloxane-terminated complex (**10**) was prepared by the hydrosilylation reaction of 1.1 equivalents of **8** with pentamethylhydrodisiloxane in toluene (Scheme 3) using a 3–3.5% solution of platinum(0) divinyltetramethyldisiloxane complex (Karstedt's catalyst) in xylene [Fluorochem] as the catalyst at room temperature, monitoring the disappearance of the Si–H stretch at 2167 cm^{-1} in the IR spectrum [6]. The product was obtained by recrystallisation from dichloromethane/methanol (1:1) as red–brown needles in 72% isolated yield. A similar procedure was used in the preparation of the dimeric complex (**11**) using complex **8** (from ligand **6b**) and 1,1,3,3-tetramethyldihydrodisiloxane (TMDS) in the molar ratio of 2:1, under the same reaction conditions. Complex **11** was isolated as a red–brown solid in 64% yield. The elemental analyses are somewhat inaccurate in the siloxane materials. This is common in these types of materials because of problems in combustion: it should be remembered that these types of materials are often used as a precursor to ceramics.

The ^{1}H NMR spectra of the **10** and **11** were clean and show that addition of the Si–H bond to the olefin is regiospecific, only the linear isomer being formed by α-addition as observed previously [6]. However, in the high field region (ca. 0.0 ppm) of **11** a number of singlets were observed, some of them partially overlapped. The relative integration of this peak was determined as 12 protons which is consistent with the stoichiometry of the pure material. We have interpreted this splitting as an indication that the fully and partly bent disiloxane conformers are present in solution together with the conformer where the tetramethyldisiloxane moiety is present in the fully extended form.

2.2. Thermo-optical properties

The mesomorphic properties of the materials were investigated by a combination of thermo-optical polarized light microscopy using an Olympus BH-2 polarized light microscope together with a Mettler FP52 microfurnace and FP5 temperature controller. The temperature controller was calibrated to an accuracy of ± 0.1°C in the range 50–285°C. Phase transitions were confirmed by differential scanning calorimetry (DSC) using a Perkin Elmer DSC2 with TADS data acquisition system at a scan rate of $\pm 10°$ min^{-1}. The instrument was calibrated against pure indium metal (Mp = 156.6°C, $\Delta H = 28.5$ J g^{-1}) [9]. The transition temperatures of the complexes studied are summarized in Table 1.

All three ligands, **6a–c**, showed no mesomorphism, melting directly to the isotropic liquid. This can be rationalized by the fact that the ethylenediamine linking group is saturated so the molecular core is unconjugated and therefore each unsymmetrical half of the molecule is free to rotate independently of the other. Furthermore, unlike 1,3-diketonate ligands which are held together in a rigid, mesogenic structure by intra-molecular hydrogen bonding, ligands **6** possess two protons in the central cavity which results in steric crowding. Single crystal X-ray diffraction studies on related ligands show that there is an anti-conformation of the substitutions about the 1,2-diamino bridge [10], a conformation not conducive to mesomorphic behavior. However, addition of a divalent metal ion has a templating effect, bringing the two halves of the molecule together to form a rigid central core with an NN′OO′ donor set. This results in the appearance of a smectic A (SmA) mesophase in all the complexes studied.

Complex **7** (from **6a**) contains a terminal *n*-alkane moiety and is therefore not activated towards hydrosilylation, but is a reference for the remaining complexes. Complex **7** exhibits a single enantiotropic smectic A (SmA) phase over the temperature range 193–221°C. The nature of the liquid crystalline phase was determined using thermo-optical polarized light microscopy. The smectic A phase was identified via its focal-conic optical texture and the low viscosity of the material at

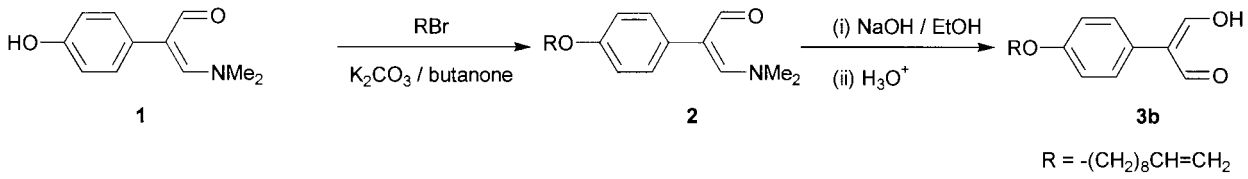

Scheme 1. Synthesis of the 4-substituted phenyl malonaldehyde.

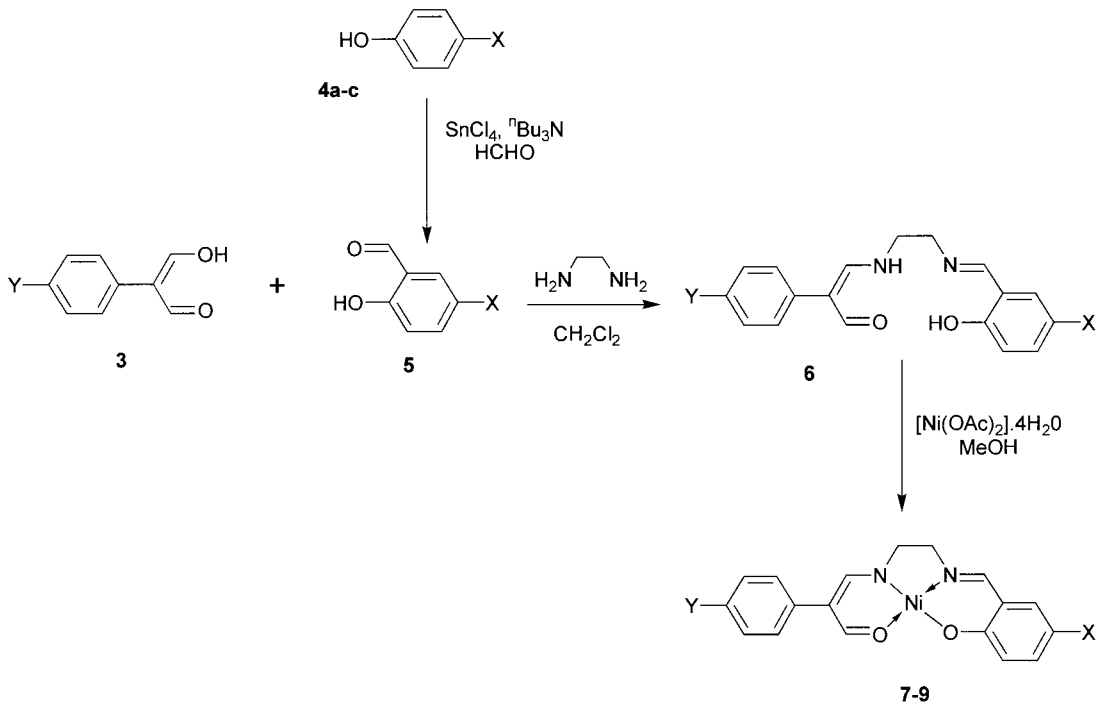

Scheme 2. General synthesis of the non-symmetric ligands and complexes. **3a**: Y = H. **3b**: Y=CH_2 =$CH(CH_2)_8O$–. **5a**: X = –$O(CH_2)_8CH_2CH_3$. **5b**: X = –$O(CH_2)_8CH{=}CH_2$. **5c**: X = H. **6a**: Y = H; X = –$O(CH_2)_8CH_2CH_3$. **6b**: Y = H; X = –$O(CH_2)_8CH{=}CH_2$. **6c**: Y = CH_2 =$CH(CH_2)_8O$–; X = H. **7**: Y = H; X = –$O(CH_2)_8CH_2CH_3$. **8**: Y = H; X = –$O(CH_2)_8CH{=}CH_2$. **9**: Y = CH_2 =$CH(CH_2)_8O$–; X = H.

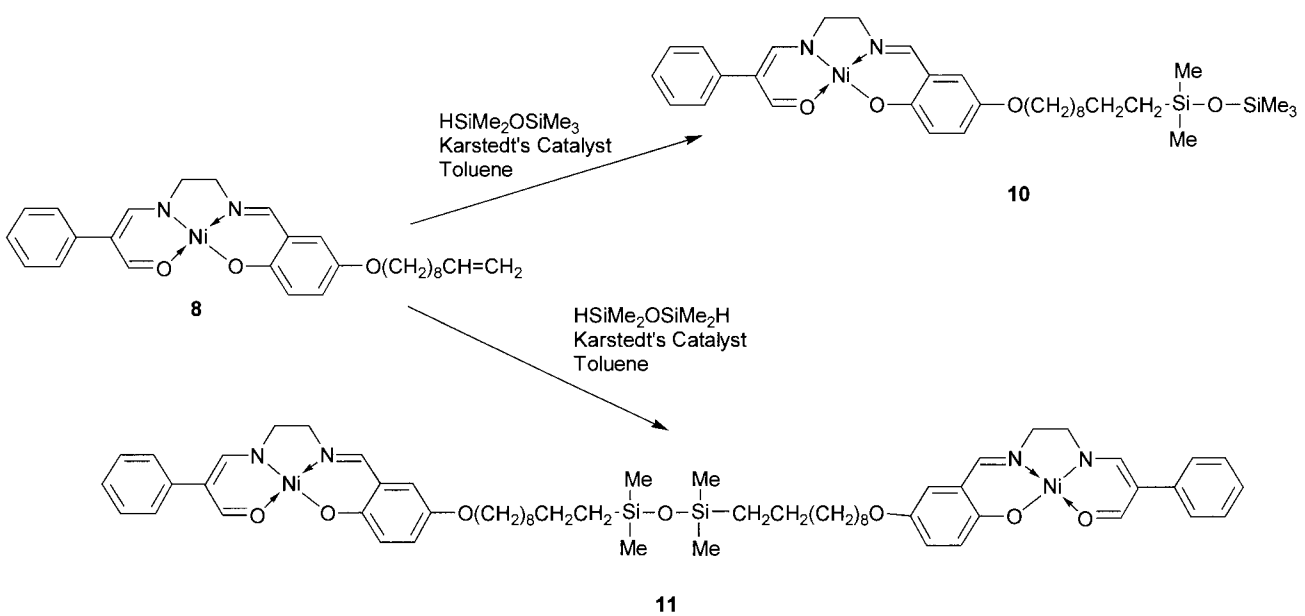

Scheme 3. Hydrosilylation reactions of monomer **8**.

Table 1
Mesomorphism in the liquid crystalline nickel complexes

Complex	X	Y	T/°C
7	$-O(CH_2)_8CH_2CH_3$	H	Cryst 193 SmA 221 Iso
8	$-O(CH_2)_8CH=CH_2$	H	Cryst 181 SmA 190 Iso
9	H	$-O(CH_2)_8CH=CH_2$	Cryst 209 Iso
10	$-O(CH_2)_{10}SiMe_2OSiMe_3$	H	$Cryst_1$ 162 $Cryst_2$ 184 SmA 240 Iso
5 (dimer)	N/A	N/A	Cryst 176 SmA 220 Iso

Mesomorphism in the non-symmetrical nickel complexes.

that temperature. For a material of similar structure but with a terminal alkenic group in the alkyl chain (**8**), then the melting point is reduced slightly but the mesophase is heavily destabilized with clearing occurring at 190°C. This observation concurs with previous experimental results for inorganic and organic materials with liquid crystalline cores [11,12].

Hydrosilylation of **8** with pentamethylhydrodisiloxane using Karstedt's catalyst (platinum(0)divinyltetramethyldisiloxane complex) at room temperature gives the complex with a terminally substituted PMDS group (**10**). This results in an increase in the melting point of 3°C with respect to the parent complex (**8**) while the clearing temperature is enhanced by 50°C, to give a smectic A phase over a 56°C temperature range. This is unexpected for the following reasons: Although for simple organic liquid crystals, introduction of a PMDS moiety tends to produce low melting point materials relative to the alkane terminated analogues, the clearing temperatures are also reduced [2]. Additionally, the PMDS unit has little effect on the melting or clearing points of the alkene terminated organic materials with

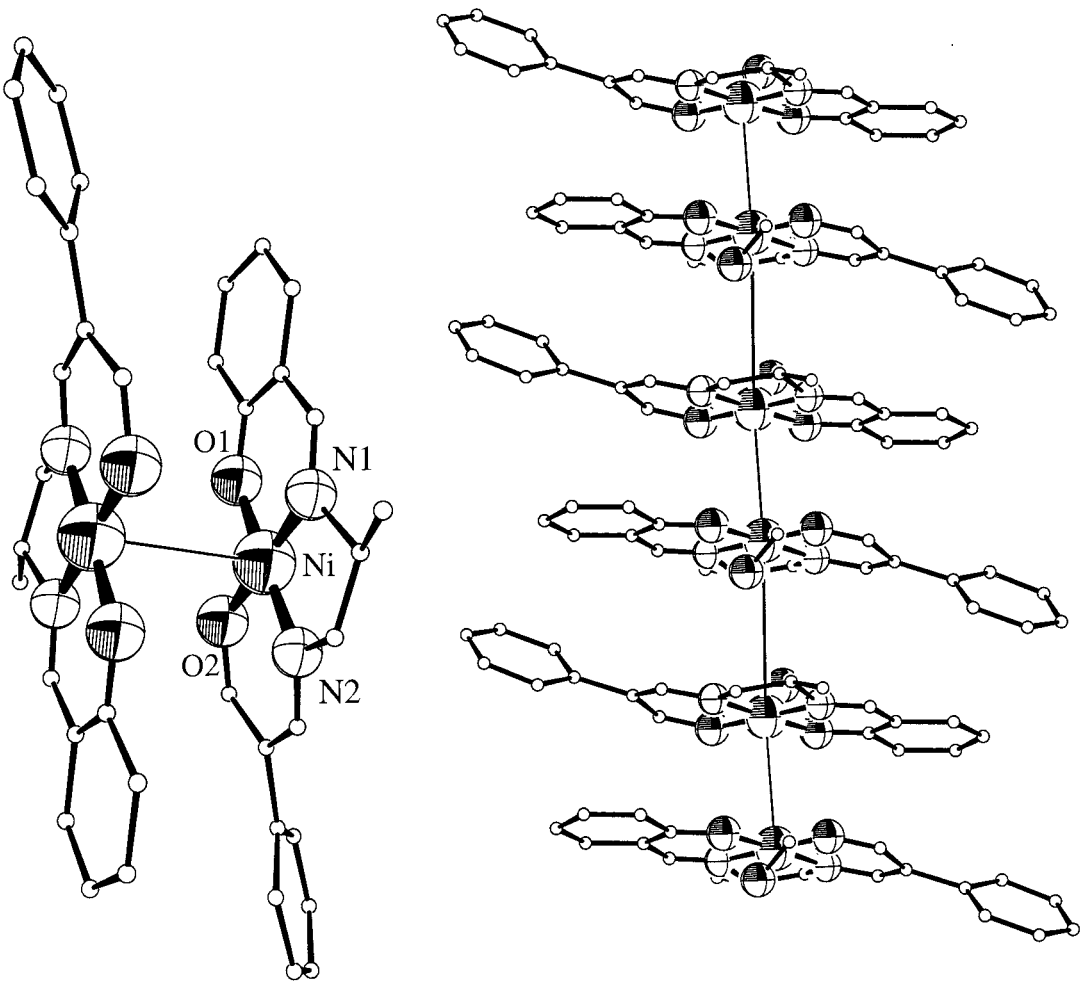

Fig. 1. ORTEP diagrams of an unsymmetrical nickel complex showing (a) dimer formation in one unit cell and (b) long range nickel–nickel interactions in the molecular structure.

long chain lengths. However, in the case of **10**, while the melting point is reduced relative to **7** but is relatively unaffected relative to **8**, the clearing temperature is substantially increased relative to both.

In order to understand the structural influence of reversing the substitution pattern on mesophase formation, we substituted the phenyl malonaldehyde sub-unit in the 4-position while keeping the salicylaldehyde sub-unit unsubstituted. The resulting alkene terminated complex **9** (from **6c**), which has the same molecular formula as **8**, showed no mesomorphism melting directly to the isotropic liquid at 209°C.

Hydrosilylation of two equivalents of **8** with diactivated 1,1,3,3-tetramethyldihydrodisiloxane yielded the dimeric TMDS complex (**11**). The dimer shows both a reduced melting point and a reduced clearing temperature relative to the monomeric PMDS complex (**10**), to give a smectic A phase with a 44°C phase range. This is again in contrast to the simple organic liquid crystalline TMDS dimers where both the melting and clearing temperature are significantly enhanced relative to the PMDS monomers [3,4].

2.3. X-ray diffraction

While the complexes described in this paper show a number of similarities to simple organic liquid crystals there are some effects that are unique and may be attributed to the presence of a transition metal center. Single crystal X-ray diffraction [2] of the non-liquid crystalline complex (**12**)

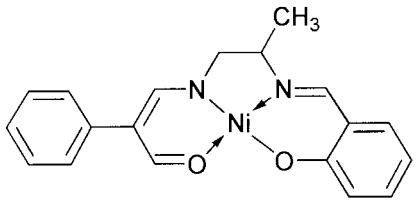

12

shows the molecules to form weakly associated dimers in the solid state [10]. The observed unweighted and weighted agreement factors were $R = 0.062$ and $R_w = 0.063$, respectively. Two discrete intermolecular nickel to nickel distances are observed which also represent the closest intermolecular contacts, with values of 3.3 and 4.3 Å. While these do not represent covalent bonds, they do represent significant interactions. The 3.3 Å separation represents the formation of weakly associated dimers (Fig. 1a) while the 4.3 Å separation is a long-range interaction between the dimeric pairs. The molecular packing diagram (Fig. 1b) shows that there is long range correlation between nickel centers, brought about by overlap of the d_z^2 orbitals, to give an extended molecular axis in the solid state. The individual molecules within the dimer are inverted relative to each other so that the different substituents are oriented at 180° to each other. While the nickel atoms may be superimposed on top of each other, the nitrogens in the chelate core from one molecule are aligned with the oxygens in the second molecule and vice versa as shown in the ORTEP diagram (Fig. 1a). Similar molecular packing is observed in the single crystal structures of similar, symmetrical mesomorphic salicylaldamine complexes that show nickel–nickel interactions over considerable correlations lengths to give an extended metallic axis [13]. This may explain the high transition temperatures observed in the liquid crystalline complexes. Unfortunately, it has not yet been possible to grow single crystals of X-ray quality for complexes **7–11**.

The dramatic change in mesophase stability as a result of a small modification in the molecular structure may be attributable to the geometry of the central chelating core. This is based on single crystal X-ray diffraction studies of unsubstituted, non-symmetric complexes [10]. The single crystal structure of complex **12**, illustrates why the reversed complex (**9**) is non-mesomorphic. The presence of the 1,2-diaminoethane bridge precludes conjugation of the molecular core so that the two aromatic sections are not co-planar. Indeed, there is a considerable twist of the phenyl malonaldehyde section away from the rest of the core. Molecular modelling of a single molecule at 400 K using constant NVT molecular dynamics with 0.001 ps time steps [CERIUS[2] ver 2.0 from Molecular Simulations (MSI)] has been used to investigate the effects of substitution of the phenyl malonaldehyde unit and also the salicylaldehyde unit. Modelling was performed on single molecules or weakly associated dimers on isolated lattice sites. Initial molecular mechanics calculations using the Universal 1.02 force field [14] were performed to minimize the energy of the initial structure. Constraints were imposed around the metal core to prevent deviations away from the observed crystal structure. Being on an isolated lattice site, interactions of neighboring molecules are neglected. The resultant simulated structures were compared with the single crystal structure using the molecular similarity routine in Cerius[2] and showed a low standard deviation around the chelation core. The chelation core is almost bowlic in nature. Substitution of the salicylaldehyde group gives a complex in which the peripheral chain is largely co-linear with the chelation core. Dimer formation gives an extended molecular geometry to form a rod-like structure that is conducive to mesophase formation. Substitution

[2] The single crystal X-ray diffraction data for **12** have been deposited with the Cambridge Crystallographic Data center and are available as supplementary data.

of the phenyl malonaldehyde unit on the other hand leads to a distorted shape that is accentuated in the dimer. The peripheral chains are not co-linear giving a distorted X-like structure that is not conducive to mesophase formation. We propose that dimer formation may be necessary for mesophase formation based on information obtained from related oxovanadium(IV) complexes. Infra red studies show the oxovanadium(IV) complexes to be completely monomeric with no evidence of metal–metal or metal–axial oxygen interactions in the solid state or in solution [15]. In contrast to the nickel complexes, these materials show no mesomorphism whatsoever, which therefore supports the assumption that dimer formation is necessary to enhance anisotropy. No X-ray data are available for these complexes at the present time although in related 1,3-diketonato complexes the closest intermolecular V…O contact is almost 8 Å, which precludes dimer formation.

In order to further characterize the nature of the smectic A phase and to derive a model for the assembly of the molecules within that phase, complexes **7**, **8** and **10** were investigated using small angle X-ray scattering (SAXS). High flux synchrotron radiation was employed so that thermal degradation of the samples did not become a problem. The experimental set-up of station 8.2 at Daresbury Laboratories [16,17] was used in order to discount the presence of a $S_A^{\sim}$ phase which is characterized by an undulation of the layer planes: a structural feature for which, in organic materials, periodicities greater than 100 Å have been observed. However, in the materials reported here, this structural feature could not observed for periodicities up to 230 Å.

Samples were prepared as polycrystalline powders in Lindemann tubes and kept at a controlled temperature. This allowed for the recording of diffraction data whilst performing temperature scans in the temperature interval of interest. The selected experimental set-up was limited to the recording of data relating to lattice parameters greater than 17.8 Å and the use of wet rat tail collagen as calibration standard leads to a systematic error of 3% in the observed *d*-spacings [18]. The systematic error is due to the sample to detector distance calibration by a natural product [16,17]. Wide angle X-ray scattering (WAXS) data are not available at the present time due to technical problems during data collection, although we intend to continue these studies.

Data were collected for the alkenyl terminated complex (**8**) on heating in the temperature interval 180 to 200°C and on cooling between 200 and 160°C. For the crystalline state preceding the transition to the smectic A phase, a *d*-spacing of 27.3(4) Å was detected. After passing through a short biphasic region, the smectic A phase was reached, where a *d*-spacing of 26.4(4) Å was observed. The recorded transition temperature of 180°C with a biphasic area up to 182°C is consistent with results observed by optical polarising microscopy and by DSC measurements. Upon reaching the liquid-crystalline state the diffraction pattern coalesced into a meridional maximum, which is indicative of some macroscopic alignment of the material via interactions with the surface of the capillary, diminishing with increased temperature, indicative of a loss of the initially obtained macroscopic ordering in the liquid crystalline state.

The overall length of **8** was calculated as 27.2 Å by molecular dynamics simulation of a single molecule (NVT, 400 K, 0.001 ps) in Cerius^2 (MSI.). This assumed that all sp^3 hybridized atoms existed in an anti-conformation about rotable bonds to give the fully extended structure, taking no account of *gauche* bonds or chain disorder. It is therefore difficult to rationalize the observed *d*-spacing in the smectic A phase with a monolayer structure. The high transition temperatures may be rationalized via a degree of assembly within the layers where weak nickel–nickel interactions are maintained after melting from the crystalline state to the mesophase. The low viscosity observed under the optical polarising light microscope suggests that the nickel–nickel interactions are present in the mesophase, but are weak in order to allow for a fluid, dynamic structure with free diffusion between layers. Above 196°C the material reached its isotropic liquid state leading to the absence of small angle intensity maxima.

Cooling the sample lead to the formation of the liquid crystalline phase at 193°C and the onset of crystallization at 179°C. Whereas the *d*-spacings in the smectic A phase were similar to those observed on heating (26.4(4) Å), the values for the crystalline phase were found to be slightly higher (27.6(4) Å). Additionally, after the onset of supercooled crystallisation two maxima were observed. One of them decreased in intensity with decreasing temperature and could be detected down to 161°C, corresponding to the smectic A phase with a *d*-spacing of 26.4(4) Å. This occurred within a biphasic region having a width of 2°C, with the crystalline state growing in to the smectic A phase.

For the alkane substituted complex (**7**), an essentially similar liquid crystalline phase structure could be observed in the temperature interval of 190 to 220°C with a *d*-spacing of 27.0(4) Å, increasing to 27.6(4) Å preceding the isotropisation temperature. As the corresponding molecular length obtained from molecular dynamics is 27.5 Å, it can be concluded that the smectic A phase is of similar structure to that proposed for **8**.

The pentamethylsiloxane substituted complex (**10**) was studied over the temperature interval 180 to 270°C, scanned at 3°C/min whilst recording diffraction data. Two maxima were observed at *d*-spacings of 35.4(6) Å on melting to the smectic A phase and at 35.9(6) Å prior to isotropisation. The values of the *d*-spacings, are slightly larger than that of the calculated maximum length of 32.2 Å obtained by molecular dynamics,

indicating that some overlap of the terminal siloxane groups placed at the interfaces between the mesogenic layers occurs. This observation is in agreement with previous experimental results for cyanobiphenyl mesogens [3,4].

2.4. A model for the smectic A phase

The alkane terminated complex (**7**) shows a *d*-spacing of 27.6 Å in the smectic A phase. The molecular length of **7** with a fully extended, all-*trans* peripheral chain was calculated as 27.2 Å using NVT molecular dynamics at a simulation temperature of 400 K. A nickel–nickel associated dimeric structure based on **7** would give an extended molecular length of ca. 37 Å. Allowing for interdigitation of the peripheral chains, containing at least one *gauche* bond, gives a structure with a calculated *d*-spacing which is in good agreement with the experimental value. This classifies the phase as a bilayer smectic A (SmA_d) phase with respect to the monomer. The interdigitation allows for good packing of the peripheral chains, leaving the bulk free of spatial voids. A similar model may be applied to the unsaturated analogue (**8**) which shows a *d*-spacing of 26.4 Å in the smectic A phase, with a calculated molecular length of ca. 36 Å for the dimer. The depression of transition temperatures observed for the unsaturated analogue is well known for simple organic liquid crystals, especially where the unsaturated moiety is situated at the chain terminus. For complexes **7** and **8** there is only a 10°C depression of the melting point on the introduction of unsaturation. This may highlight the role of the metal center on phase stabilisation although further studies are required in this area. For all the complexes investigated in this study the difference in the melting points was found to be surprisingly small. There is, however, a 30°C depression of the clearing temperature of **8** relative to **7**. This can be directly related to the presence of the terminal alkene, which can cause packing difficult in the smectic A phase and so destabilized the structure.

The inclusion of a pentamethyldisiloxane end group (**10**) has little effect on the melting point of the complex relative to complex **8**, but shows a similar depression (10°C) relative to the saturated analogue (**7**). However, the clearing point of **10** is increased significantly relative to both complexes **7** and **8**. This effect is unusual in pentamethyldisiloxane terminated materials. A model to explain such phase behaviour is shown in Fig. 2. An intercalated phase structure of the SmA_d-type, based on pairing the of single molecules of **10**, would require a *d*-spacing of 41 Å in the fully extended form (Cerius^2). The observed stabilisation of the smectic A phase of the organosiloxane containing material with respect to the alkyl or alkenyl terminated mesogen may be attributable to the existence of weak nickel–nickel interactions, having a templating-like effect to aid layer formation. It has been proposed that the organosiloxane end groups self-organize through polar interactions to produce a layered structure in the smectic A phase, separated into organosiloxane, hydrocarbon and aromatic sub-regions [2–4,6]. Calculations on isolated molecules of **10** and its related dimeric structure to determine the electrostatic potential over the surface of the molecule were performed in WebLab Viewer ver 2.0.1 (MSI) using the surface generator with a probe diameter of 1.4 Å. The electrostatic surfaces of a single molecule or a weakly associated dimer, which had previously been simulated at 400 K using NVT molecular dynamics (Cerius^2) reveal that the organosiloxane region, rather than being a highly polar moiety, is considerably non-polar. Regions of high electron density are clearly visible around the chelation core and around the oxygen of the ether side chain. An unexpected feature of the organosiloxane region is the steric shape of the group, which exhibits a kidney-like shape that allows for an off-center packing of like-groups. This dissymmetry allows for the self-organisation of the organosiloxane moieties into a sub-layer as shown in Fig. 2, which in turn results in a high degree of interdigitation, and allows for good space filling. The resulting calculated layer spacing corresponds well with the experimental *d*-spacing (35.4 Å) as shown in Fig. 2. It may be possible to attribute the stabilisation of the mesophase to the increased ordering of the molecules in the phase brought about by self-organisation of the organosiloxane end groups, which require increased energy for breakdown. Further studies

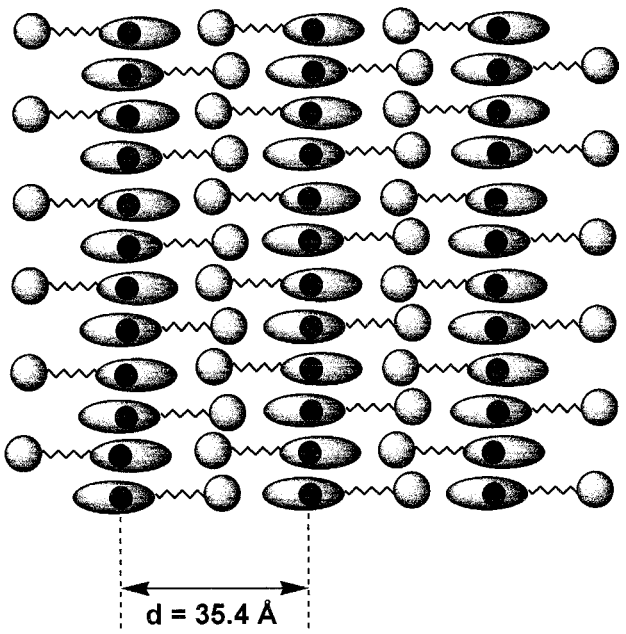

Fig. 2. A model for the smectic A phase in the PMDS terminated complex. Nickel atoms are shown as black circles (●). The larger grey circles represent the off-set PDMS units.

are in progress on a range of different materials in an attempt to fully clarify the phase structure.

We propose that the existence of dimeric molecules is necessary to support mesophase formation as the monomeric molecules themselves do not possess a sufficiently mesogenic structure, being substituted on only one side of the central chelation core. We would point to the loss of mesomorphism in the oxovanadium(IV) complexes discussed earlier [15] as evidence for this. The differences in melting points are brought about as a direct result of the packing abilities of the terminal moieties and are consistent with previously reported systems. The differences in clearing temperatures however, are reasonably unique. In simple cyanobiphenyl liquid crystal systems [2–4], inclusion of a pentamethyldisiloxane unit tends to give a large depression of the melting and clearing temperatures with respect to the alkyl-terminated material. The melting and clearing points of the PMDS-terminated cyanobiphenyls are however relatively unchanged with respect to the alkenyl-terminated analogues. However, for the material reported here, the clearing temperature is significantly increased on the inclusion of a pentamethyldisiloxane unit relative to both the alkyl and alkenyl terminated analogues. We therefore propose that the clearing temperature corresponds to the breakdown of the dimeric nickel–nickel interactions to form discreet monomeric units. It should be pointed out that the model is consistent with the assembly of the sub-units in terms of their associated 'philicities'.

3. Experimental

Solvents were dried over appropriate drying agents and distilled prior use. Nickel acetate tetrahydrate was purchased from Aldrich and used as received. All siloxane materials, including Karstedt's catalyst were purchased from Fluorochem.

Infrared spectra were recorded on a Perkin–Elmer 783 spectrometer. NMR spectra were recorded on a Jeol JNM-GX spectrometer (^{1}H, 270 MHz); chemical shifts are reported in parts per million (δ) with reference to internal $SiMe_4$ or residual protonated species of the deuterated solvent used for ^{1}H analysis. Elemental analysis was performed on a Fisons Instruments Carlo Erba EA 1108 CHN analyzer using acetanilide as the reference standard. V_2O_5 was added to aid combustion in a number of cases. Mass spectra were recorded on a Finnigan 1020 GC-MS spectrometer (electron ionisation mode/70 eV) and on a Kratos MS80 spectrometer (fast atom bombardment mode/NOBA matrix).

3.1. 2-(4-Dec-9-enyloxyphenyl)-N,N-dimethyl-1-aminoprop-1-en-3-al, (2)

(4-Hydroxyphenyl)dimethylaminoacrolein (**1**) (3.00 g, 15.6 mmol), K_2CO_3 (2.49 g, 18.0 mmol) and $C_{10}H_{19}Br$ (3.26 g, 14.9 mmol) in butanone (200 ml) were heated to reflux (20 h), protected from moisture with a calcium chloride guard tube. The resulting suspension was filtered off and the solution evaporated to dryness to yield a white solid. The solid was purified by column chromatography (flash grade silica gel; elution with CH_2Cl_2/THF 4/1), to yield **2** as a colorless syrup ($R_f = 0.54$). Yield = 4.89 g (94%).

3.2. (4-Dec-9-enyloxy)phenyl malonaldehyde, (3a)

A solution of sodium hydroxide (7.42 g, 185 mmol) in water (22 ml) was added to a solution of **2** (4.89 g, 14.84 mmol) in ethanol (100 ml) and the two layer mixture heated gently to reflux for 3 h. The solution was cooled down to room temperature and the ethanol evaporated in vacuo until only water remained. The white solid so formed was filtered off, suspended in water (100 ml) and the strongly alkaline solution was neutralized with 10N HCl until ca. pH 3. The resulting white solid was filtered off, washed repeatedly with water, dissolved in CH_2Cl_2 and the organic layer dried over $MgSO_4$. The solvent was evaporated and the white solid produced was recrystallised form petroleum ether. Yield = 3.18 g (71%).

^{1}H NMR ($CDCl_3$): δ 14.30 (s, 1H, OH); 8.70 (s, 2H, CHO, =CH–OH); 7.17, 6.92 (AB q, 4H, aromatic); 5.81 (d(J_{trans} = 17 Hz) d(J_{cis} = 10 Hz) t(J_{fg} = 7 Hz), 1H, CH_2=C*H*); 4.99 (d(J_{trans} = 17 Hz) m, 1H, H^e); 4.93 (d(J_{cis} = 10 Hz) m, 1H, H_d); 3.87 (t(J = 7 Hz), 2H, CH_2O); 2.04 (m, 2H, CH_2–CH=); 1.73 (m, 2H, CH_2–CH_2–O); 1.30 (m, 10H, $(CH_2)_5$).

3.3. 4-(Decyloxy)phenol, (4a)

Hydroquinone (37.65 g, 342 mmol) and 1-bromodecane (23.65 ml, 114 mmol) were dissolved in ethanol (150 ml) with warming under a nitrogen atmosphere. The solution was heated under reflux and a solution of potassium hydroxide (6.83 g, 121 mmol) in water (20 ml) was added dropwise over 1 h. The resulting suspension was heated under reflux (3 h) then poured on to water (500 ml) and extracted with ether (3 × 100 ml). The combined extracts were dried ($MgSO_4$), evaporated in vacuo and the residue extracted with heptane (300 ml). Cooling afforded a first crop of the phenol (10.31 g). The remaining material was chromatographed (flash grade silica gel, petroleum ether 40–60°C/diethyl ether 3/2). **2** was isolated as white plates ($R_f = 0.57$). Combined yield = 15.69 g (55%). Mp = 54°C.

^{1}H NMR ($CDCl_3$): δ 6.76 (m, 4H, aromatic); 4.63 (s, 1H, OH); 3.88 (t(J = 7 Hz), 2H, CH_2O); 1.74 (m, 2H, CH_2–CH_2O); 1.30 (m, H, $(CH_2)_7$), 0.70 (t(J = 7 Hz), 3H, CH_3).

3.4. 4-(Dec-9-en-yloxy)phenol (4b)

The synthetic procedure was as described for 4a above using the following quantities: Hydroquinone

(37.65 g, 342 mmol); dec-9-enylbromide (25 g, 114 mmol); potassium hydroxide (6.83 g, 121 mmol). Yield = 15.61 g (55%). Mp = 54°C.

^{1}H NMR ($CDCl_3$): δ 6.78 (m, 4H, aromatic); 5.81 (d(J_{trans} = 17 Hz) d(J_{cis} = 10 Hz)t(J_{fg} = 7 Hz), 1H, CH_2=C*H*); 4.99 (d(J_{trans} = 17 Hz) m, 1H, H_e); 4.93 (d(J_{cis} = 10 Hz) m, 1H, Hd); 4.63 (s, 1H, O*H*); 3.89 (t(J = 7 Hz), 2H, CH_2O); 2.04 (m, 2H, CH_2–CH=); 1.73 (m, 2H, CH_2–CH_2–O); 1.30 (m, 10H, (CH_2)5).

3.5. 2-Hydroxy-5-(decyloxy)benzaldehyde, (5a)

$SnCl_4$ (0.52 ml, 4.53 mmol) was added to a solution of 4-decyloxyphenol (11.35 g, 45.3 mmol) in sodium dried, degassed toluene (250 ml) under a dry nitrogen atmosphere. Tri-*n*-butylamine (4.30 ml, 18.13 mmol) was added at room temperature. The solution turned yellow and was stirred for 1 h before paraformaldehyde (BDH) (2.99 g, 100 mmol) was added and the yellow suspension heated to 105°C (3 h). The brown solution was cooled, poured onto saturated aqueous NaCl (200 ml) and acidified to pH 2 with 10% HCl. The product was extracted with ether (3 × 100 ml) and the combined organic layers dried ($MgSO_4$) and evaporated. The residue was purified by column chromatography (flash grade silica gel; petroleum ether 40–60°C/diethyl ether, 3/2). The title compound **5a** was isolated as a yellow oil (R_f = 0.62). Yield = 3.72 g (29%).

^{1}H NMR ($CDCl_3$): δ 10.64 (s, 1H, O*H*); 9.85 (s, 1H, C*H*O); 7.13 (d(J_{ab} = 9 Hz) d(J_{bc} = 3 Hz), 1H, H_b); 7.00 (t(J = 3 Hz), 1H, Hc); 6.92 (d(J = 9 Hz), 1H, Ha); 3.94 (t(J = 7 Hz), 3H, CH_2O); 1.78 (m, 2H, CH_2–CH_2–O); 1.60 (m, 14H, $(CH_2)_7$); 0.88 (t(J = 7 Hz), 3H, CH_3).

3.6. 2-Hydroxy-5-(dec-9-enyloxy)benzaldehyde, (5b)

The preparation was as described above for compound **5a** using the following quantities: $SnCl_4$ (0.27 ml, 2.33 mmol), 4-(dec-9-enyloxy)phenol (5.80 g, 23.33 mmol), toluene (250 ml), tri-*n*-butylamine (2.22 ml, 9.34 mmol), paraformaldehyde (1.54 g, 51 mmol). The title compound **5b** was isolated as a yellow oil (R_f = 0.62). Yield = 2.44 g (38%).

^{1}H NMR ($CDCl_3$): δ 10.91 (s, 1H, O*H*); 9.85 (s, 1H, C*H*O); 7.32 (d(J = 3 Hz), 1H, H_a); 7.24 (m, 1H, H_b); 7.0 (d(J = 9 Hz), 1H, H_c); 5.81 (d(J_{trans} = 17 Hz) d(J_{cis} = 10 Hz) t(J_{fg} = 7 Hz), 1H, CH_2=C*H*); 4.99 (d(J_{trans} = 17 Hz) m, 1H, He); 4.93 (d(J_{cis} = 10 Hz) m, 1H, H_d); 3.87 (t(J = 7 Hz), 2H, CH_2O); 2.04 (m, 2H, CH_2–CH=); 1.73 (m, 2H, CH_2–CH_2–O); 1.30 (m, 10H, (CH_2)$_5$).

3.7. 8-(3-Decyloxy-6-hydroxyphenyl)-2-phenyl-4,7-diazocta-2,7-dien-1-al, (6a)

1,2-Diaminoethane (0.33 ml, 5 mmol) was added to a vigorously stirred solution of phenylmalonaldehyde (0.74 g, 5 mmol) in dichloromethane (300 ml). A white precipitate formed immediately. The salicylaldehyde **5a** (1.391 g, 5 mmol) was added and the resulting suspension stirred at room temperature (18 h) and then refluxed using a Dean–Stark apparatus until a clear yellow solution was obtained (6 h). The yellow solution was evaporated in vacuo and the residue purified by column chromatography (flash grade silica gel, Cl_2CH_2/THF, 4/1). The band with R_f = 0.83 yielded symmetrical salen derivative (0.369 g, 51%). The band with R_f = 0.66 was collected and the product recrystallized from Cl_2CH_2/MeOH to yield yellow microcrystals of **6a**. Yield = 0.616 g (55%). The percentage yields are based on the statistical maximum theoretical yields: (50% maximum for the unsymmetrical ligand and 25% maximum for the salen ligand in the reaction mixture) [6].

Microanalysis: Calcd for $C_{28}H_{38}O_3N_2$: C, 74.64; H, 8.49; N, 6.21. Found: C, 74.46; H, 8.74; N, 6.11.

MS (EI): *m*/*z* 451(M) 450 ($M^+ - 1$); 421 (M^+ – CO).

^{1}H NMR (CDCl3): δ 12.57 (s, 1H, O*H*); 10.60 (m broad, 1H, N*H*); 9.60 (d(J = 4 Hz), 1H, C*H*O); 8.43 (s, 1H, C*H*=N); 7.45-6.87 (m, 9H, aromatic C_6H_5, H_a, H_b, H_c, NC*H*=C); 4.01 (t(J = 7 Hz), 2H, CH_2O); 3.93 (m, 2H, CH_2–N=CH); 3.78 (m, 2H, CH_2–NH); 1.85 (m, 2H, CH_2–CH_2–O); 1.40 (m, 14H, (CH_2)7); 0.95 (t(J = 7 Hz), 3H, CH_3).

3.8. 8-(3-Dec-9-enyloxy-6-hydroxyphenyl)-2-phenyl-4,7-diazocta-2,7-dien-1-al, (6b)

1,2-Diaminoethane (0.2 g, 3.36 mmol) was added to a vigorously stirred solution of 2-phenyl-3-hydroxypropenal (0.498 g, 3.36 mmol) in CH_2Cl_2 (300 ml). A white precipitate formed immediately. 2-Hydroxy-5-(dec-9-enyloxy)benzaldehyde (0.93 g, 3.36 mmol) was added and the yellow suspension was stirred at room temperature (18 h) and then heated under reflux (5 h) using a Dean–Stark apparatus protected from moisture with a calcium chloride guard tube. The yellow solution was evaporated in vacuo and the residue purified by column chromatography (flash grade silica gel; CH_2Cl_2/THF, 4/1). The band with R_f = 0.76 yielded the symmetrical by-product 1,6-di(3-dec-9-enyloxy-6-hydroxyphenyl)-2,5-diazahexa-1,5-diene after recrystallisation from ethanol (yield = 0.19 g, 40%). The band with R_f = 0.50 was collected and the product recrystallised from ethanol to yield bright yellow crystals of **6b**. Yield = 0.46 g (61%) [6].

Micro analysis: Calc. for $C_{28}H_{36}O_3N_2$: C, 74.97; H, 8.08; N, 6.24. Found: C, 74.66; H, 8.12; N, 6.21.

MS (EI): *m*/*z* 448 (M^+); 420 (M^+ – CO). ^{1}H NMR ($CDCl_3$): δ 12.45 (s, 1H, OH); 10.48 (m broad, 1H, NH); 9.47 (d(J = 4 Hz), 1H, C*H*O); 8.31 (s, 1H, C*H*=N); 7.30-6.72 (m, 9H, aromatic C_6H_5, H_a, H_b, H_c, NC*H*=C); 5.81 (d(J_{trans} = 17 Hz) d(J_{cis} = 10

Hz)t(J_{fg} = 7 Hz), 1H, CH_2=C*H*); 4.99 (d(J_{trans} = 17 Hz) m, 1H, H_e); 4.93 (d(J_{cis} = 10 Hz) m, 1H, H_d); 3.88 (t(J = 7 Hz), 2H, CH_2O); 3.81 (m, 2H, CH_2–N=CH); 3.65 (m, 2H, CH_2–NH); 2.04 (m, 2H, CH_2–CH=); 1.70 (m, 2H, CH_2–CH_2–O); 1.30 (m, 10H, (CH_2)$_5$).

3.9. 8-(2-Hydroxyphenyl)-2-(4-dec-9-enyloxy-6-hydroxyphenyl)-4,7-diazocta-2,7-dien-1-al, (6c)

The reversed ligand was prepared as described previously for **6ac** from **3b** (1.209 g; 4.0 mmol), 1,2-diaminoethane (0.26 ml; 4.0 mmol) and salicylaldehyde (Aldrich) (0.41 ml; 4.0 mmol) in CH_2Cl_2. Yield = 0.155 g (17%).

Microanalysis: Calcd for $C_{28}H_{36}O_3N_2$: C, 74.97; H, 8.08; N, 6.24. Found: C, 75.33; H, 8.23; N, 6.23.

MS (EI): m/z 448 (M^+).

^{1}H NMR ($CDCl_3$): δ 12.95 (s, 1H, OH); 10.37(m broad, 1H, N*H*); 9.40 (d(J = 4 Hz), 1H, C*H*O); 8.36 (s, 1H, C*H*=N); 7.40-6.78 (m, 9H, aromatic C_6H_4, NC*H*=C); 5.82 (d(J_{trans} = 17 Hz) d(J_{cis} = 10 Hz)t(J_{fg} = 7 Hz), 1H, CH_2=C*H*); 4.99 (d(J_{trans} = 17 Hz) m, 1H, H_e); 4.93 (d(J_{cis} = 10 Hz) m, 1H, H_d); 3.91 (t(J = 7 Hz), 2H, CH_2O); 3.79 (m, 2H, CH_2–N = CH); 3.62 (m, 2H, CH_2–NH); 2.04 (m, 2H, CH_2–CH=); 1.70 (m, 2H, CH_2–CH_2–O); 1.30 (m, 10H, (CH_2)$_5$).

3.10. [8-(3-decyloxy-6-hydroxyphenyl)-2-phenyl-4,7-diazocta-1,3,7-trienato](2-) nickel(II), (7)

Nickel acetate tetrahydrate (99.5 mg; 0.4 mmol) was added to a solution of **6a** (0.180 g; 0.4 mmol) in methanol (15 ml) heated to reflux. A mass of red crystals formed immediately. The suspension was heated to reflux for 1 h. After cooling to room temperature, the red needles formed were filtered off and recrystallized from methanol. Yield = 0.163 g (80%).

Mesomorphism: Cryst 193 SmA 221 Iso °C.

Microanalysis: Calcd for $C_{28}H_{36}O_3N_2Ni$: C, 66.30; H, 7.14; N, 5.51. Found: C, 66.17; H, 7.02; N, 5.39.

MS (EI): m/z 508 ($M^+ + 1$); 506 ($M^+ - 1$); 365 ($M^+ - C_{10}H_{19}$).

IR (KBr disc, υ cm^{-1}): 1609 (vs, sharp; C=N, C=O and C=C–N coordinated).

^{1}H NMR ($CDCl_3$): δ 7.45-7.10 (m, 8H; aromatic C_6H_5, *H*C=N, *H*C=O and NC*H*=C); 6.93 (m, 2H, H_a, H_b); 6.52 (m, 1H, H_c); 3.82 (t(J = 7 Hz), 2H, CH_2O); 3.38 (m, 2H, CH_2–N=CH); 3.31 (m, 2 H, CH_2–NH); 1.72 (m, 2H, CH_2–CH_2–O); 1.30 (m, 14H, (CH_2)$_7$); 0.89 (t(J = 7 Hz), 3H, CH_3).

3.11. [8-(3-Dec-9-enyloxy-6-hydroxyphenyl)-2-phenyl-4,7-diazocta-1,3,7-trienato](2-) nickel(II), (8)

A suspension of nickel acetate tetrahydrate (0.1941 g, 0.78 mmol) in methanol (5 ml) was added to a solution of **6b** (0.350 g, 0.78 mmol) in methanol (30 ml) which was heated to reflux. The red solution obtained was heated under reflux (1 h) and on cooling to room temperature produced red–brown needles which were filtered off, dried and recrystallized from methanol. Yield = 0.355 g (90%).

Mesomorphism: Cryst 181 SmA 190 Iso °C.

Microanalysis: Calcd for $C_{28}H_{34}O_3N_2Ni$: C, 66.56; H, 6.77; N, 5.54. Found: C, 66.47; H, 6.65; N, 5.46.

MS (EI): m/z 504 ($M^+ - 1$); 365 ($M^+ - C_{10}H_{19}$).

Molecular weight determination (osmometry in $CHCl_3$): Calcd for $C_{28}H_{34}O_3N_2Ni$: 505.24; Found: 567.

IR (KBr disc, υ/cm^{-1}): 1609 (vs, sharp; C=N, C=O and C=C–N coordinated).

^{1}H NMR ($CDCl_3$): δ 7.4-7.0 (m, 8H; aromatic C_6H_5, *H*C=N, *H*C=O and NC*H*=C); 6.91 (m, 2H, H_a,H_b); 6.48 (m, 1H, H_c); 5.81 (d(J_{trans} = 17 Hz)d(J_{cis} = 10 Hz)t(J_{fg} = 7 Hz), 1H, CH_2=C*H*); 4.99 (d(J_{trans} = 17 Hz)m, 1H, H_e); 4.93 (d(J_{cis} = 10 Hz)m, 1H, H_d); 3.79 (t(J = 7 Hz), 2H, CH_2O); 3.34 (m, 4H, NCH_2); 2.04 (m, 2H, CH_2–CH=); 1.70 (m, 2H, CH_2–CH_2–O); 1.30 (m, 10H, (CH_2)$_5$).

3.12. 8-(2-Hydroxyphenyl)-2-(4-dec-9-enyloxy-6-hydroxyphenyl)-4,7-diazocta-1,3,7-trienato](2-) nickel(II), (9)

Nickel(II) acetate tetrahydrate (24.8 mg; 0.1 mmol) was added to a refluxing solution of **6c** (44.8 mg; 0.1 mmol) in methanol (10 ml). Red plates formed immediately. The red suspension was heated (1 h), cooled down to room temperature and the red crystals filtered off and dried in air. Yield = 28.7 mg (57%). Mp = 209°C.

Microanalysis: Calcd for $C_{28}H_{34}O_3N_2Ni$: C, 66.56; H, 6.77; N, 5.54. Found: C, 65.10; H, 6.66; N, 5.37. Calcd for $C_{28}H_{34}O_3N_2Ni.CH_3OH$: C, 64.81; H, 7.13; N, 5.24.

MS (EI): m/z 504 ($M^+ - 1$); 365 ($M^+ - C_{10}H_{20}$).

IR (KBr disc, υ cm^{-1}): 1609 (vs, sharp; C=N, C=O and C=C–N coordinated).

^{1}H NMR ($CDCl_3$):7.48-6.80 (m, 10H, C_6H_4 aromatic, *H*C=N, *H*CO, NC*H*=C); 6.53 (m, 1H, aromatic); 6.53 (m, 1H, H_c); 5.81 (d(J_{trans} = 17 Hz)d(J_{cis} = 10 Hz)t(J_{fg} = 7 Hz), 1H, CH_2 = C*H*); 4.99 (d(J_{trans} = 17 Hz)m, 1H, H_e); 4.93 (d(J_{cis} = 10 Hz)m, 1H, H_d); 3.92 (t(J = 7 Hz), 2H, CH_2O); 3.37 (m, 2H, CH_2–N=C*H*); 3.30 (m, 2H, CH_2–NH); 2.04 (m, 2H, CH_2–CH=); 1.70 (m, 2H, CH_2–CH_2–O); 1.30 (m, 10H, (CH_2)$_5$).

3.13. [8-(2-Hydroxy-5-(10-(1,1,3,3,3-pentamethyldisiloxy)decyloxy)phenyl)-2-phenyl-4,7-diazocta-1,3,7-trienato](2-) nickel(II), (10)

10 μl of 3–3.5% solution of Karstedt's catalyst (platinum(0) divinyldisiloxane complex) in xylene (Flu-

orochem) was added to a solution of nickel(II) complex **8** (0.1731 g, 0.342 mmol) in toluene (8 ml) under a dry nitrogen atmosphere. The solution was stirred (1 h) at room temperature and a solution of pentamethylhydrodisiloxane (Fluorochem) (44.1 mg, 0.297 mmol) in toluene (5 ml) was added dropwise over a period of 1 h. IR spectral monitoring of the reaction showed complete disappearance of the Si–H band in 2–4 h. The red solution was stirred overnight and the solvent removed in vacuo. The residue was dissolved in CH_2Cl_2 (5 ml), passed down a short pasteur pipette loaded with Hyflo (Filter Aid) and the red solution layered with methanol (80 ml) to yield red–brown needles which were recrystallized from CH_2Cl_2/MeOH once more to afford **10** as red–brown needles. Yield = 0.14 g (72%).

Mesomorphism: $Cryst_1$ 164 $Cryst_2$ 184 SmA 240 Iso (°C).

Microanalysis: Calcd for $C_{33}H_{50}O_4N_2NiSi_2$: C, 60.64; H, 7.70; N, 4.28. Found: C, 62.01; H, 7.55; N, 4.39.

Table 2
Experimental details for the structure determination of **12**

A. Crystal data	
Empirical formula	$C_{20}H_{22}O_3N_2Ni$
Crystal color, habit	red, prism
Crystal dimensions (mm)	0.60×0.33×0.20
No. reflections used for unit Cell determination	25
Omega scan peak width at half-height	0.40
Lattice parameters	a = 7.332(3) Å b = 23.604(7) Å c = 10.689(4) Å β = 94.60(5) V = 1844(2) 3
Space Group	$P2_1/c$
Z value	4
μ(MoK α)	10.76 cm^{-1}
B. Intensity measurements	
Diffractometer	Rigaku AFC6S
Radiation	MoK α (λ = 0.71069)
Temperature	21°C
Scan type	$\omega - 2\theta$
Scan rate	8°/min (in ω)
$2\theta_{max}$	54.1°
No. of reflections measured	Total 4486, unique 4171
Corrections	Lorentz-polarization, absorption (trans. factors: 0.69–1.32) decay (−9.20% decline)
C. Structure solution and refinement	
Structure solution	Heavy atom (Patterson)
Refinement	Full-matrix least-squares
Function minimized	$\Sigma w(\|F_o\| - \|F_c\|)^2$
Least-squares weights	$4F_o^2/\sigma^2$ (F_o^2)
p-factor	0.03
No. observations ($F_0^2 > 3\ \sigma(F_0^2)$)	1287
No. variables	205
Residuals: R; R_w	0.062; 0.063
Goodness of fit indicator	1.91

Table 3
Positional parameters and B(eq) for **12**

Atom	x	y	z	B(eq)
Ni	0.2058(2)	0.01025(6)	0.9511(1)	3.42(6)
O(1)	0.1371(9)	0.0827(3)	0.9003(6)	4.0(4)
O(2)	0.1486(9)	−0.0092(3)	0.7847(6)	.1(3)
O(3)	0.248(2)	0.1089(5)	0.654(1)	13(1)
N(1)	0.267(1)	0.0293(3)	1.1164(8)	3.7(4)
N(2)	0.282(1)	−0.0609(4)	0.9920(8)	3.3(4)
C(1)	0.189(1)	0.1277(5)	1.098(1)	4.0(2)
C(2)	0.134(1)	0.1276(4)	0.970(1)	3.6(2)
C(3)	0.065(1)	0.1784(5)	0.915(1)	5.0(3)
C(4)	0.064(1)	0.2275(5)	0.985(1)	5.4(3)
C(5)	0.125(2)	0.2281(5)	1.107(1)	6.2(3)
C(6)	0.190(2)	0.1798(5)	1.163(1)	5.2(3)
C(7)	0.258(1)	0.0786(5)	1.161(1)	4.6(6)
C(8)	0.344(2)	−0.0191(6)	1.190(1)	9(1)
C(9)	0.351(2)	−0.0164(6)	1.329(1)	7.0(8)
C(10)	0.321(2)	−0.0710(5)	1.128(1)	6.0(8)
C(11)	0.308(1)	−0.1043(5)	0.920(1)	4.2(6)
C(12)	0.272(1)	−0.1030(5)	0.788(1)	3.8(6)
C(13)	0.192(2)	−0.0552(6)	0.730(1)	4.9(7)
C(14)	0.330(1)	−0.1510(5)	0.712(1)	3.9(6)
C(15)	0.320(2)	−0.2059(5)	0.756(1)	4.8(6)
C(16)	0.391(2)	−0.2512(5)	0.693(1)	5.8(7)
C(17)	0.462(2)	−0.2420(7)	0.578(1)	6.0(8)
C(18)	0.468(2)	−0.1876(7)	0.534(1)	6.4(8)
C(19)	0.400(2)	−0.1430(5)	0.597(1)	4.8(6)
C(20)	0.111(3)	0.092(1)	0.563(1)	15(2)
H(O)	0.2350	0.0862	0.7718	13.7
H(3)	0.0181	0.1778	0.8300	6.2
H(4)	0.0231	0.2614	0.9450	6.6
H(5)	0.1282	0.2612	1.1531	7.4
H(6)	0.2299	0.1799	1.2502	6.2
H(7)	0.2963	0.0839	1.2489	5.3
H(8)	0.4871	−0.0154	1.1777	11.7
H(11)	0.3584	−0.1371	0.9578	5.2
H(13)	0.1527	−0.0571	0.6408	5.6
H(14)	0.2663	−0.2129	0.8323	5.5
H(15)	0.3832	−0.2887	0.7258	6.5
H(16)	0.5164	−0.2727	0.5375	6.4
H(17)	0.5134	−0.1837	0.4536	7.3
H(18)	0.4091	−0.1067	0.5592	5.1
H(21)	−0.0078	0.0999	0.5865	16.9
H(22)	0.1260	0.1132	0.4851	16.9
H(23)	0.1205	0.0529	0.5424	16.9
H(91)	0.3814	0.0198	1.3585	7.3
H(92)	0.2345	−0.0276	1.3550	7.3
H(93)	0.4406	−0.0433	1.3651	7.3
H(101)	0.2153	−0.0859	1.1627	10.7
H(102)	0.4137	−0.0986	1.1494	5.4

MS (EI): m/z 652 ($M^+ - 1$); 504 ($M^+ - (CH_3)_3Si-O-Si(CH_3)_2$); 365 ($M^+ - (CH_3)_3Si-O-Si(CH_3)_2C_{10}H_{20}$); 349 ($M^+ - (CH_3)_3Si-O-Si(CH_3)_2C_{10}H_{20}O$).

IR (KBr disc; υ, cm^{-1}): 1608 (vs, sharp; C=N, C=O and C=C–N coordinated); 1057 (vs, broad; Si–O–Si).

^{1}H NMR(CD_2Cl_2): δ 7.43 (s, 1H), 7.28 (m. 3H), 7.14 (m, 4H, aromatic Ph, HC=N, HC=O, N–CH=C); 6.87 (d(J_{ab} = 9 Hz)d(J_{bc} = 3 Hz), 1H, H_b); 6.71 (d(J_{ab} = 9 Hz), 1H, H_a); 6.54 (d(J_{bc} = 3 Hz) 1H, H_c); 3.80

(t(J = 6 Hz) 2H, CH_2O); 3.30 (m, 4H, CH_2N); 1.69 (m, 2H, CH_2–CH$_2$O); 1.30 (m, 14H, (CH_2)$_7$); 0.49 (m, 2H, CH_2–Si); 0.04 (s, 9H, (CH_3)$_3$Si–O); 0.01 (s, 6H, CH$_2$–(CH_3)$_2$ Si–O).

3.14. Bis{[8-(2-hydroxy-5-(dec-10-yl-1-yloxy)phenyl)-2-phenyl-4,7-diazocta-1,3,7-trienato](2-) nickel(II)}-1,1,3,3-tetramethyldisiloxane, (**11**)

5 μl of 3–3.5% solution of Karstedt's catalyst in xylene was added to a solution of nickel(II) complex **8** (44 mg; 0.008 mmol), in toluene (8 ml) under a dry nitrogen atmosphere. The solution was stirred (1 h) at room temperature and a solution of tetramethyldihydrodisiloxane (Fluorochem) (5.69 mg, 0.004 mmol) in toluene (1 ml) was added at once. IR spectral monitoring of the reaction showed complete disappearance of the Si–H band. The red solution was stirred overnight and the solvent removed in vacuo. The residue was dissolved in CH$_2$Cl$_2$ (5 ml), passed down a short pasteur pipette loaded with Hyflo (Filter Aid) and the red solution evaporated under vacuo; the red solid obtained was washed with a little toluene, diethyl ether and dried under vacuum. Yield = 31 mg (64%).

Mesomorphism: Cryst 176 SmA 220 Iso °C.

Microanalysis: Calcd for $C_{60}H_{82}O_7N_4Ni_2Si_2$: C, 62.95; H, 7.21; N, 4.89. Found: C, 62.05; H, 7.09; N, 4.80.

MS (FAB): m/z 1145 (M^+), 827, 535, 505, 365.

IR (KBr disc; υ, cm^{-1}): 1608 (vs, sharp; C=N, C=O and C=C–N coordinated); 1096-1037 (vs, broad; Si–O–Si).

^{1}H NMR (CD$_2$Cl$_2$): δ 7.44 (s, 1H), 7.33-7.08 (m, 7H, aromatic Ph, HC=N, HC=O, N–CH=C); 6.88 (d(J_{ab} = 9 Hz)d(J_{bc} = 3 Hz), 1H, H_b); 6.69 (d(J_{ab} = 9 Hz), 1H, H_a); 6.55 (d(J_{bc} = 3 Hz) 1H, H_c); 3.81 (t(J = 6 Hz) 2H, CH_2O); 3.32 (m, 4H, CH_2N); 1.69 (m, 2H, CH_2–CH$_2$O); 1.30 (m, 14H, (CH_2)$_7$); 0.49 (m, 2 H, CH_2–Si); 0.10-0.01 (several singlets; 6H, CH$_2$–(CH_3)2–Si–O).

3.15. Structure determination of **12**

All measurements were made as previously described [19] on a red prismatic crystal mounted on a glass fiber. The experimental details are summarized in Table 2. The metal atom position was determined from a 3-D Patterson function based on all data. This phased the data sufficiently to locate the other atoms from difference Fourier maps. Most of the non-hydrogen atoms were refined anisotropically. Full-matrix least-squares refinement was carried out using the TEXRAY [20] program set, giving unweighted and weighted agreement factors of:

$$R = \frac{\Sigma||F_o| - |F_c||}{\Sigma|F_o|} = 0.062$$

$$R_w = \left[\frac{\Sigma w(|F_o| - |F_c|)^2}{\Sigma wF_o^2}\right]^{\frac{1}{2}} = 0.063$$

The standard deviation of an observation of unit weight 6 was 1.91.

Tables 3 and 4 give the atomic fractional coordinates and selected interatomic distances and angles, respectively. The molecular structure consists of a neutral Ni(II) complex with a methanol sovate hydrogen-bonded to the phenolic oxygen of the unsymmetrical ligand. The metal environment is approximately planar with each of the donor atoms deviating less than 0.02 Å from the least squares plane through the first co-ordination sphere. The Sal ligand ring O(1)–C(2)–C(1)–C(7)–N(1) is coplanar with this plane, as is the phenolic ring. The main deviation comes from the other donor ring O(2)–C(13)–C(12)–C(11)–N(2) at 10.2° and the attached phenyl at 41.4° to the plane of the first co-ordination sphere. The closest intermolecular approach (3.308 Å)

Table 4
Selected interatomic distances and angles for **12**

Atom	Atom	Distance	Atom	Atom	Distance (Å)
Ni	Ni′	3.308(3)(a)	Ni	O(2)	1.852(6)
Ni	Ni″	4.383(3)(b)	Ni	N(1)	1.844(8)
Ni	O(1)	1.851(6)	Ni	N(2)	1.813(7)
Intermolecular distances					
O(1)	O(3)	2.88(1)(a)	O(2)	O(3)	3.22(1)(a)
O(1)	C(10)	3.36(2)(b)	O(2)	N(1)	3.34(1)(b)

Symmetry operators: (a) x, y, z; (b) $-x, -y, 2-z$; (c) $1-x, -y, 2-z$

Atom	Atom	Atom	Angle	Atom	Atom	Atom	Angle (°)
O(1)	Ni	O(2)	84.9(2)	Ni	O(1)	C(2)	127.2(5)
O(1)	Ni	N(1)	95.4(3)	Ni	O(2)	C(13)	127.0(6)
O(1)	Ni	N(2)	176.2(3)	Ni	N(1)	C(7)	125.1(7)
O(2)	Ni	N(1)	179.1(3)	Ni	N(1)	C(8)	111.9(6)
O(2)	Ni	N(2)	92.6(3)	Ni	N(2)	C(10)	114.7(6)
N(1)	Ni	N(2)	87.0(3)	Ni	N(2)	C(11)	130.1(7)

is between the nickel atoms of adjacant molecules. The pairs of molecules have their nickel atoms separated by 4.383 Å from each other to form alternating short and long Ni–Ni separations along an infinite Ni . . . Ni . . . . Ni . . . Ni . . . . chain.

Acknowledgements

Dr. Peter Styring is the first DRA Lecturer in Chemistry. We wish to thank the EPSRC for funding (IMS) in the form of a PDRA (Grant reference No: K/08567). We gratefully acknowledge everyone at the University of Hull Analytical Services (Brenda Worthington, Alan D. Roberts and Carol Kennedy) for help in the materials' characterisation and to the University of Sheffield for the provision of FAB mass spectra (Simon Thorpe) and osmometry (Sue Bradshaw). We would also like to express thanks to Dr. B.U. Komanschek at Daresbury Laboratories for his support and help in the SAXS studies.

References

[1] J.L. Serrano (Ed.), Metallomesogens, VCH, Weinheim, 1996.
[2] J. Newton, H. Coles, P. Hodge, J. Hannington, J. Mater. Chem. 4 (1994) 869.
[3] M. Ibn-Elhaj, A. Skoulios, D. Guillon, J. Newton, P. Hodge, H. Coles, Liq. Cryst. 19 (1995) 373.
[4] M. Ibn-Elhaj, A. Skoulios, D. Guillon, J. Newton, P. Hodge, H. Coles, Journal de Physique II 3 (1993) 1807.
[5] P. Styring, I.M. Saez, N. Gough, E. Sinn, J.W. Goodby, Patent application No. 9613068.7 (filed 21 June 1996).
[6] I.M. Saez, P. Styring, Adv. Mater. 8 (1996) 1001.
[7] I.M. Saez, P. Styring, Mol. Cryst. Liq. Cryst., (1997) in press.
[8] D. Lloyd, C. Reichardt, M. Struthers, Liebigs Ann. Chem. (1986) 1368.
[9] O. Kubaschewski, E.L. Evans, Metallurgical Thermochemistry, 4th edn., Pergamon, New York, 1958.
[10] I.M. Saez, P. Styring, A.N. Paterson, E. Sinn, in preparation.
[11] P. Maldivi, L. Bonnet, A.M. Giroud-Godquin, M. Ibn-Elhaj, D. Guillon, A. Skoulios, Adv. Mater. 5 (1993) 909.
[12] S.M. Kelly, Liq. Cryst. 20 (1996) 443.
[13] A.B. Blake, J.R. Chipperfield, W. Hussain, R. Paschke, E. Sinn, Inorg. Chem. 34 (1995) 1125.
[14] A.K. Rappe, W.A. Goddard III, J. Phys. Chem. 95 (1991) 3358.
[15] I.M. Saez, P. Styring, in preparation.
[16] W. Bras, G.E. Derbyshire, D. Bogg, J. Cooke, M.J. Elwell, B.U. Komanschek, S. Naylor, A.J. Ryan, Science 267 (1995) 996.
[17] W. Bras, J. Bouwstra, NIMPR A326 (1993) 587.
[18] W. Folkhard, W. Geercken, E. Knoerzer, E. Mosler, H. Nemetschek-Gansler, T. Nemetschek, M.H.J. Koch, J. Mol. Biol. 193 (1987) 405.
[19] J.R. Backhouse, H.M. Lowe, E. Sinn, S. Suzuki, S. Woodward, J. Chem. Soc., Dalton Trans. (1995) 1489.
[20] TEXSAN–TEXRAY Structure Analysis Package, Molecular Structure (1985).